CORONA DISCHARGE USED AS AN ION SOURCE FOR AEROSOL CHARGING

A. BOUAROURI[1*], N.JIDENKO[1], J.-P. BORRA[1], F.GENSDARMES[2], D.MARO[2], D.BOULAUD[2]

[1] *Laboratoire de Physique des Gaz et des Plasmas, Équipe Décharges Électriques et Aérosols (CNRS – Université Paris XI F-91405), Supelec F-91192, France*

[2] *Institut de Radioprotection et de Sûreté Nucléaire, BP 68, 91192, Gif-sur-Yvette, France*

*assia.bouarouri@u-psud.fr

ABSTRACT

To develop a "real time" aerosol sizer, a post-corona charger is studied. Aerosol charging depends mainly on $N_i.\tau$ product (N_i is the ion density and τ is the charging time) and on the aerosol diameter. The time devoted to charging is shorter than 0.1 s. To compensate this short time, mean ion densities of about 10^8 cm^{-3} are required. At first, geometrical and electrical parameters of the corona discharge are chosen to achieve a stable ion production and quasi-stationary ion density profiles in the charger. Then, the ion extraction to reach such post-discharge ion density is optimized. Since the mixing of ions with aerosol is critical for post-discharge ion distribution and so for $N_i.\tau$ product "seen" by the aerosol, two mixing arrangements are compared. Indeed, it is confirmed that the final number of elementary charge collected by the aerosol depends on the mixing.

1. INTRODUCTION

To evaluate the effect of particulate pollutants on the environment, dry deposition rate of aerosol (solid and liquid particles suspended in a gas) has to be estimated. To do so, a method based on eddy covariance between aerosol size distribution (from 10 nm to 1µm with concentration between 10^3 and 10^5 cm^{-3}) and wind velocity at 10 Hz has recently been developed [1]. Commercial aerosol sizers for atmospheric aerosol have a response time of about 1 s. This work aims to develop a device with a response time of 0.1 s by electrical methods. Indeed, within 0.1 s, the aerosol can be charged by ion collection, separated according to mobilities of suspended particles related to their size for charged aerosol current measurement. From these currents per mobility range, the aerosol concentration for each size range can be estimated.

Electrical discharges are often used to produce ions for aerosol charging [2-5]. Gas injection in the discharge gap is used to blow ions from the gap throw a hole in the earthed electrode into the post-discharge charging zone [5].

The mean number of charges per particle depends on aerosol diameter and on the $N_i.\tau$ product with N_i, the mean ion density and τ, the transit time. Since charging should be shorter than 0.1s, mean ion densities of about 10^8 cm^{-3} are required to reach measurable charged aerosol currents. To reach such mean ion density in the charger, the initial unipolar ion density has to be in the order of 10^{10} cm^{-3} at the inlet of the charging zone, since it decreases by 4 orders of magnitude in 0.1 s by electrostatic repulsions [5].

Here, the chargers are characterized in terms of discharge current and regimes as well as in terms of ion extraction controlling the initial ion density in the post-discharge aerosol charger. Finally, preliminary size–charge relations are depicted for two ion-aerosol mixing conditions.

2. EXPERIMENTAL SETUP

The experimental set-up is presented in Figure 1.

Clean and dry air is injected in the discharge to extract ions towards the post-discharge aerosol charger.

The discharge current is measured to control the ion production as well as the output current (I_{out}) to evaluate the initial ion density in the post-discharge aerosol charger. This ion density is estimated with the output current (I_{out}) and the gas flow rate (Q_{ion}). It's given by:

$$N_{ion}^{o} = \frac{I_{out}}{e.Q_{ion}}$$

with e, the elementary charge.

Calibrated aerosol (monodisperse size with known diameter and concentration) is produced and injected into the charging zone.

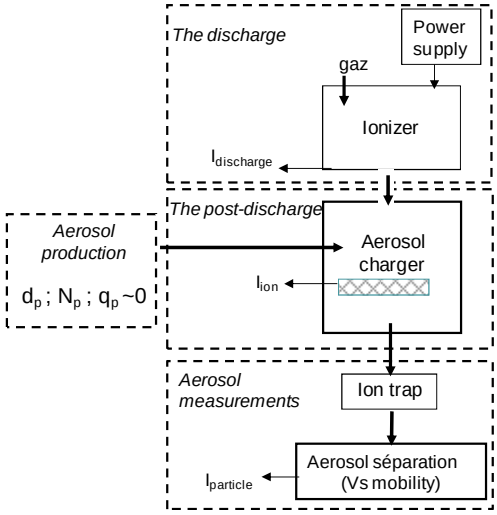

Figure 1: Experimental setup

Aerosol is produced with different generators. For aerosol, size of 10 to 100 nm, NaCl aerosol is produced by a furnace while 300-900 nm oil droplets are produced by a Sinclair-LaMer generator (SLG).

Downstream the charging zone, an ion trap collects residual ions for accurate measurements of the electrical charge imparted to particles versus their diameter and concentrations without ions. The measurements of particle concentration upstream (N^{in}, using a Condensation Particle Counter) and downstream the charger (N^{out}, using a particle counter sizer -PCS-) gives the penetration of the charger (N^{out}/N^{in}). Furthermore, the mean number of charges per particle is derived from:

$$< q_p >= \frac{I_{aerosol}}{e.Q_{electrometer}.N^{out}}$$

with $I_{aerosol}$, the current of charged particles, $N_{aerosol}$, the aerosol concentration downstream the charger and $Q_{electrometer}$, the flow rate sampled by the electrometer.

3. RESULTS

3.1 ION PRODUCTION: CORONA DISCHARGE

Positive ions are produced by gas ionization and negative ions by electron attachment. These processes depend on the nature of the gas and on the reduced electric field E/N, with E, the electric field and N, the gas density. The electric field depends on the applied voltage (V), the point radius (R_c) and the gap length (d_{gap}). The point is polarized by a negative voltage. Indeed, negative ions mobility is higher than the positive ones. Thus, charging velocity in the same ion density is higher with negative ions. The effect of electrical and geometrical parameters is studied to achieve a constant initial ion density and a quasi-stationary ion density profiles in the post-discharge charger.

I(V) characteristics for both geometries are shown in Figure 1. For wire-to-slit arrangement, the discharge current per unit of length (J) is plotted versus the applied voltage. The length of the wire is L=20 mm.

For the point-to-hole arrangement, the stable regimes are the Trichel and the Corona regimes. In the Trichel regime, high frequency (100 kHz) current pulses of about 100 ns occur and the average current variation is less than 5% [7]. For higher voltages, the Corona regime leads to a continuous current.

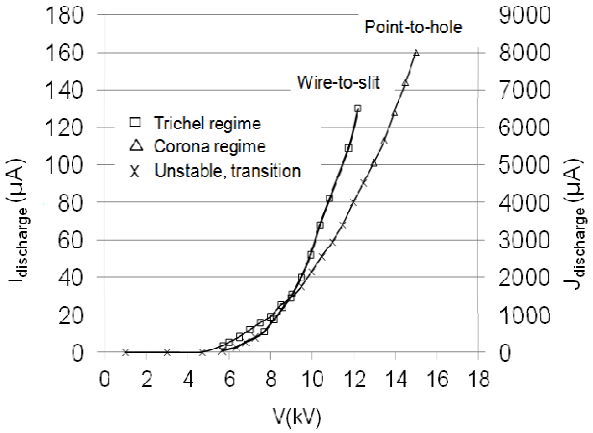

Figure 2 : I(V) characteristics for point-to-hole (R_c=80 µm, d=13 mm, P=1.020 bar, Q_{ion}= 30 lpm) and wire-to-slit (R_c=100 µm, d= 6 mm, L=20 mm, P=1020 mbar, Q_{ion}= 30 lpm)

A point radius of 80 µm has been chosen, with a gap length of 13 mm for a pressure of 1 to 1.3 bar to achieve at least 2 kV of voltage range with stable Trichel and Corona regimes.

For wire-to-slit arrangement with a wire radius of 100 µm and a gap length of 6 mm, the only stable regime is the Trichel one from 8 to 12 kV.

3.2 POST-DISCHARGE ION CURRENTS

The initial ion density in the post-discharge aerosol charger is controlled by the discharge current and the competition between electrostatic forces which induce ion losses on the walls and hydrodynamic forces in the discharge gap as well as in the output hole.

In the hole, this electro-hydrodynamic competition is controlled by the ratio of two characteristic times. The drift time (t_{drift}, related to radial trajectory of ion in the hole) is the mean time required by ions to reach the walls of the hole. The drift time depends on the radial electric field (related to Laplace field from the polarized electrode, space charge and surface polarization) and the diameter of the hole. The transit time

($t_{transit}$, related to axial trajectory) is the mean time that ion would spend in the hole if there was no collection. The transit time depends on the length of the hole, the gas velocity and the axial electric field.

Then, for a metal drilled plane, ion losses on the walls of the hole can reach up to 99% of the input current entering the hole. To limit the losses, a drilled plane made of three layers: metal (50 µm)-insulator (200 µm)-metal (1 mm) is used. With this hole maximal losses are 90% and can be decreased down to 10%. Indeed, the surface polarization of dielectric walls affects the drift time. This one becomes greater than with metal walls and, as a result, ion losses are reduced.

The choice of the hole diameter is a compromise between maximal gas velocity to enhance ion extraction and minimal pressure drop below 500 mbar to limit the dimension and the cost of the pumping system. With aerosol concentration down to 10^3 cm^{-3}, electrometer sensitivity at 10 Hz down to tens of fA and singly charged aerosol, the required aerosol flow rate is estimated around 30 lpm. To charge the aerosol an excess of ion is required (N_i>1000·$N_{particle}$) so that an ion flow of the same order of magnitude than the aerosol flow is chosen (Q_{ion} = 30 lpm). From these constraints a diameter hole of 2 mm (ΔP ~ 450 mbar).

Figure 3 shows the initial ion densities extracted from point-to-hole and wire-to-slit geometries and for flow rates of 5 and 30 lpm versus the discharge current.

At first, one can note that 10^{10} cm^{-3} ion density corresponds to an initial ion current (at the entrance of the charging zone) in the order of 0.5 µA, meaning that less than 0.5 % of the discharge current is injected in the post-discharge for high discharge current (100 µA).

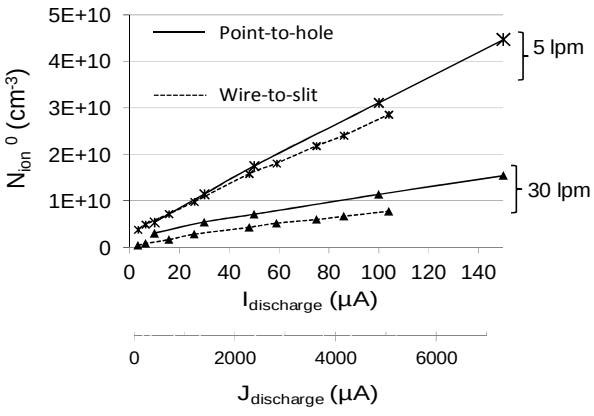

Figure 3: Extracted ion density for both point-to-hole and wire-to slit geometries

On figure 3, initial post-discharge ion density (N_{ion}°) increases linearly with the discharge current (controlled by the applied voltage), even if the extraction efficiency (not presented) decreases with increasing discharge current (due to higher ions losses in the hole). That proves that the radial electric field for ion collection increases. In our conditions, the radial space charge electric field is only partly limited by the subsequent polarization of the dielectric wall due to ion collected.

Ion density decreases with the flow rate due to dilution. However, reduced losses with shorter transit time and smaller space charge repulsion of ions in the hole at higher flow rate leads to a twice higher ion density than expected from dilution.

Similar trends are depicted for the wire-to-slit arrangements. Both ion sources produce comparable ion density with different spatial distribution of ions that will be studied to optimize aerosol charging.

If the initial ion density in the charging zone is about 10^{10} cm^{-3}, the mean ion density estimated from aerosol charge measurements is about 10^7 cm^{-3} (cf. §3.3). This is one order of magnitude lower than the estimated mean ion density required for aerosol charging in 0.1 s(cf. §1).

3.3 CHARGE-DIAMETER RELATION

To define the optimal ion-aerosol mixing conditions, perpendicular and face-to-face ion and aerosol jets are compared in terms of aerosol charge level and losses for the point-to-hole post-corona charger.

For both mixings conditions, aerosol losses are lower than 10 %. Figure 4 depicts the charge per particle for aerosol concentration of 10^4 cm^{-3}, as well as Fuchs law related to the charging of aerosol by diffusion of ions on particles versus aerosol diameter for Ni.t close to 5.10^5 cm^{-3}.s, as derived from the fitting of the mean charge for 100 nm particle.

For aerosol diameter below 200 nm, the mean number of charge per particle obtained with both mixing configurations are in adequation with Fuchs theory estimated for a mean ion density and $N_i.\tau$ =5.10^5 $s.cm^{-3}$. However, the measured mean number of charge for diameter above 200 nm differs from those calculated with Fuchs charging law using the same charging conditions (i.e. using the same Ni.τ).

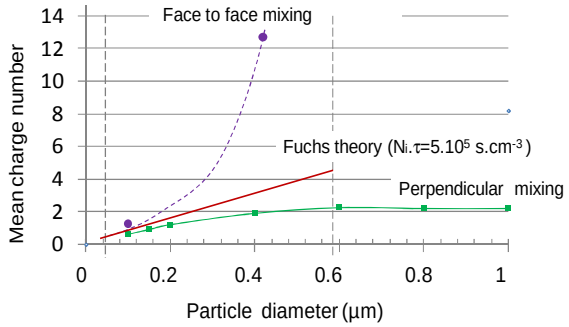

Figure 4: mean number of charge per aerosol obtained with face to face and perpendicular mixing in the point-to-hole arrangement.

Indeed, in such heterogeneous profile of unipolar ion density in the charging zone, the final charge of the aerosol depends on its path in the ion cloud. Both the ion density profiles and the aerosol trajectories are controlled by mixing conditions: relative velocities and flow rates of ions and aerosol, which are kept constant, as well as the angle between aerosol and ion jets and the aerosol size.

For perpendicular mixing and for diameters above 200 nm, the mean number of charges is almost constant. This is probably due to the lack of ions related to highly heterogeneous ion density in the charging zone, where larger particles may be swept from the aerosol jet outside the highest ion density, probably due to inertia.

For the face-to-face mixing, preliminary results show a large gap with Fuchs' theory for 460 nm particles: the mean number of charges of about 12 charges per particle is estimated against 3 charges per particle calculated with Fuchs' law. This can be attributed to higher $N_i.\tau$ "seen" by these 460 nm particles than for perpendicular jet mixing or to field charging mechanism for particles injected closer to the hole used for ion injection from the discharge gap.

4. CONCLUSION

For "real time" electrical measurements of atmospheric aerosol concentration, corona discharge is used as an ion source for aerosol charging.

Two ion sources arrangements (point-to-hole and wire-to-slit) have been characterized in terms of discharge current and regime as well as related initial post-discharge ion densities.

The working conditions to produce constant initial ion densities (~ 10^{10} cm^{-3}) with less than 5% of temporal fluctuation and a quasi-stationary decreasing ion density profiles in the post-discharge charger, have been defined for both discharge geometries.

It has been shown that the ion extraction is mainly controlled by an electro-hydrodynamic competition. As a result, ion losses in the discharge output have been reduced by the polarization of dielectric wall of the ion output by ion collection due to electrostatic repulsion. The two mixing conditions investigated for the point-to-hole arrangement illustrate two effects. For the perpendicular mixing, a lack of ions due to heterogeneous ion profile and inertial effect for larger particles can explain the low charge level measured. For the face-to-face mixing, the field charging mechanism or higher real $N_i.\tau$ for particles larger than 200 nm diameter can explain the higher charge level measured than calculated (with Fuchs' law using Ni.τ estimated from the measured mean charge level of 100 nm particle).

Other mixing arrangements still have to be studied in order to choose the optimal mixing condition for the point-to-hole as well as for the wire-to slit corona chargers to ensure high charge levels, aerosol losses below 10% and a linear relation between charged aerosol current and aerosol concentration.

REFERENCES

[1] P.E.Damay, D. Maro, A.Coppalle, E.Lamaud, O. Connan, D.Hebert, M.Talbaut. & M. Irvine, "Size-resolved eddy covariance measurements of fine particle vertical fluxes". Journal of Aerosol Science, **40,** 1050-1058, 2009.

[2] P. Intra, P. & N.Tippayawong, "An Overview of Unipolar Charger Developments for Nanoparticle Charging". Aerosol and Air Quality Research, **11,** 187-209, 2011

[3] M.Alonso, F.J. Alguacil, F. J, "Effect of ion and particle losses in a charger on reaching a stationary charge distribution". JAS, 34, 1647-64, 2003.

[4] A.Marquard, J,Meyer, "Characterization of electrical aerosol chargers: A review of charger performance criteria". JAS, 37, 1052-68, 2006.

[5] K.T. Whitby, "Generator for Producing High Concentrations of Small Ions". Rev. Sci. Instrum., **32**, 1351-1355, 1961.

[6] G.S Hewitt, "The Charging of Small Particles for Electrostatic Precipitation". AIEE Trans. 76: 300–306, 1957.

[7] G.W. Trichel, "The Mechanism of the Negative Point to Plane Corona Near Onset". Physical Review, **54,** 1078, 1938.